

1 **Revision 1:**

2 **Accurate Determination of Ferric Iron in Garnets**

3 **<sup>1</sup>Ryan J. Quinn, <sup>1</sup>John W. Valley, <sup>2</sup>F. Zeb Page, <sup>1</sup>John H. Fournelle**

4 <sup>1</sup>Dept. of Geoscience, University of Wisconsin, Madison, WI 53706

5 <sup>2</sup>Geology Department, Oberlin College, Oberlin, OH 44074

6  
7 **Abstract**

8 Numerous techniques are available to determine the amount of  $Fe^{2+}$  and  $Fe^{3+}$  in minerals.  
9 Calculating  $Fe^{2+}$  and  $Fe^{3+}$  by charge-balance using electron probe microanalysis (EPMA) data  
10 is the most common method, but several studies question the usefulness and accuracy of this  
11 approach (Canil and O'Neill, 1996; Dyar et al., 2012; Dyar et al., 1993; Lalonde et al., 1998; Li  
12 et al., 2005; McGuire et al., 1989; Schingaro et al., 2016; Schmid et al., 2003; Sobolev et al.,  
13 2011). We compile and compare data for natural garnets that have been analyzed by both EPMA  
14 and Mössbauer spectroscopy. Comparison of  $Fe^{3+}/\Sigma Fe$  determined by charge-balance vs.  
15 Mössbauer spectroscopy shows an approximate 1:1 correlation. The EPMA data set of Dyar et al.  
16 (2012) is reexamined and it is shown that disagreement between EPMA and Mössbauer for their  
17 data is not nearly as bad as reported. Data for charge-balance vs. Mössbauer spectroscopy are  
18 compared and show that the EPMA/charge-balance approach provides a suitable alternative  
19 when other methods are not practical.

20  
21 **Keywords:** Ferric iron, EPMA, Charge balance, Mössbauer spectroscopy

22  
23 **Introduction**

24 The oxidation state of iron is important to many aspects of mineralogy and petrology  
25 including thermobarometry and determination of oxygen fugacity in rocks or melts. Several  
26 methods exist for determining the ratio of  $Fe^{3+}$  to  $Fe^{2+}$ . Most commonly, it is either directly

27 measured by wet chemistry (Johnson and Maxwell, 1981; Wilson, 1960) or Mössbauer  
28 spectroscopy (Dyar et al., 2006), or calculated from electron probe microanalysis (EPMA; e.g.  
29 Valley et al., 1983; Droop, 1987; Essene, 1989; Grew et al., 2013). Other techniques including  
30 X-ray photoelectron spectroscopy (Raeburn et al., 1997a; Raeburn et al., 1997b), electron energy  
31 loss spectroscopy (Garvie and Buseck, 1998), EPMA-based ‘flank method’ (Höfer and Brey,  
32 2007), and synchrotron based X-ray absorption near-edge spectroscopy (Bajt et al., 1994) have  
33 been employed to explicitly measure the valence of iron. The EPMA/charge-balance technique is  
34 the most frequently employed because of widespread EPMA accessibility, small spot size (~ 3  
35  $\mu\text{m}$ ), and speed of analysis. Furthermore, analysis is essentially non-destructive. However, the  
36 EPMA/charge-balance approach is, in some circumstances, less precise and requires accurate  
37 analysis while making some assumptions: no vacancies, no unmeasured elements (e.g. H, Li, B),  
38 and that *Fe* is the only element with more than one valence state. Fluorine should be measured  
39 by EPMA (Valley et al., 1983). These assumptions are not met for hydrous minerals, e.g.  
40 amphiboles, micas, chlorites, hydro-garnets, and staurolites; because  $\text{H}_2\text{O}$  is not measured by  
41 EPMA (Essene, 1989). It is well known that charge balance does not yield a unique result when  
42 the assumptions fail (Droop, 1987) and we will not discuss these minerals. Instead we focus on  
43 the garnet group (excluding hydrous species where  $\text{H}_2\text{O}$  was unmeasured), where the authors  
44 believe charge-balance calculations to be a valuable tool after EPMA analysis.

45

## 46 **Methods**

47 We calculate  $Fe^{3+}/\sum Fe$  by charge-balance for garnets (Table 1) according to the following  
48 procedure:

49 1) calculate the formula from EPMA data normalized to 8 cations;

- 50 2) calculate the total charge contribution from all cations assuming all *Fe* is  $Fe^{2+}$ ;
- 51 3) a) if the total cation charge is greater than 24 (cation charge of an ideal formula), then
- 52 all *Fe* is ferrous and there is no ferric *Fe*;
- 53 b) if the cation charge is less than 24, calculate the amount of  $Fe^{3+}$  cations by
- 54 subtracting the total cation charge from 24, i.e.

$$Fe^{3+} = 24 - \sum_i C_i V_i \quad (\text{Eqn. 1})$$

56 where C is the amount of the  $i^{\text{th}}$  cation and V is the valence of the  $i^{\text{th}}$  cation;

- 57 4) a) if the amount of calculated  $Fe^{3+}$  is greater than total *Fe*, then enter zero for  $Fe^{2+}$  and
- 58 set  $Fe^{3+}$  to equal total *Fe*,
- 59 b) if the amount of calculated  $Fe^{3+}$  is less than total *Fe*, subtract the calculated  $Fe^{3+}$
- 60 from the total *Fe* to determine amount of  $Fe^{2+}$ .

61 This procedure is slightly different than that of Droop (1987), but is preferred by the authors due

62 to its simplicity. For each data set we back-calculated total *Fe* as *FeO* from reported *FeO* and/or

63  $Fe_2O_3$  and the above procedure was implemented to ensure consistency of charge balance

64 calculations. If data for  $H_2O$ ,  $Li_2O$ , or other oxides that are not typically measured by EPMA are

65 available through another method e.g. secondary ion mass spectrometry (Schingaro et al., 2016)

66 or Fourier transform infrared spectroscopy (Locock et al., 1995), then they can be combined with

67 EPMA data and incorporated into charge balance calculations according to (Grew et al., 2013).

68 The accuracy of charge-balance calculations is dependent on several factors. Counting

69 statistics during EPMA analysis provides an assessment of instrumental precision, but not of

70 accuracy. Choice of analytical standards can make critical differences for EPMA of silicates and

71 oxides, including garnets due to chemical peak shifts for Mg- and Al-K $\alpha$  between non-garnet

72 standards and sample garnets (Fournelle, 2007; Fournelle and Jonnard, 2011). Fournelle and

73 Geiger (2010) examined EPMA of synthetic grossular and pyrope, using non-garnet standards  
74 (e.g. wollastonite, corundum, Fo-rich olivine) and noted a range of errors (Al – 3% low; Mg – 1%  
75 high; Si – 1% high) and different possible analytical results that were dependent upon (1) which  
76 mass absorption coefficient and (2) which matrix correction were used. These results emphasize  
77 the need for garnets as standards, ideally for all elements, obviating any chemical peak shift and  
78 minimizing error in matrix correction.

79 Conditions of EPMA analysis and the selected standards, mass absorption coefficients,  
80 and matrix correction are not always reported resulting in data that are difficult to evaluate (e.g.  
81 Li et al., 2005). Due to the vague nature of some reports, we estimate error bars by conducting a  
82 sensitivity analysis of  $Fe^{3+}/\sum Fe$  to  $SiO_2$ . Data for Si are predicted to be the largest contribution  
83 to uncertainty in charge balance calculations because  $Si^{4+}$  is the most abundant cation and has the  
84 highest charge. For each sample,  $SiO_2$  was adjusted by  $\pm 1\%$ , then  $Fe^{3+}/\sum Fe$  was calculated by  
85 charge-balance and these values were used as endpoints for the error bars along the x-axis (Fig.  
86 1). Note that in some cases the error bars are asymmetrical due to the fact that  $Fe^{3+}/\sum Fe$  can not  
87 be less than 0 or greater than 1. If calculation of  $Fe^{3+}/\sum Fe$  after propagating both +1 and -1%  
88  $SiO_2$  result in a  $Fe^{3+}/\sum Fe$  value less than 0 (or both are greater than 1), then no error bar is  
89 shown because they do not encompass possible solutions. The uncertainty of  $Fe^{3+}/\sum Fe$   
90 calculations varies with total  $Fe$ ; at  $\sim 5$  wt% FeO(total) error in  $Fe^{3+}/\sum Fe$  is more than triple that  
91 of garnets where FeO(total) is greater than 15 wt% (Fig. 2).

## 93 Discussion

94 Several garnet studies have compared EPMA/charge-balance with other methods and in  
95 general imply that accuracy of  $Fe^{3+}/\sum Fe$  determination by charge-balance is questionable (Canil

96 and O'Neill, 1996; Dyar et al., 2012; Dyar et al., 1993; Li et al., 2005; McGuire et al., 1989;  
97 Schingaro et al., 2016; Sobolev et al., 2011). Sobolev et al. (1999) state “...*there is no direct (1:1)*  
98 *correlation between the two sets of data*” in reference to charge-balance vs. Mössbauer, but base  
99 this on 4 data with  $Fe^{3+}/\sum Fe$  less than 0.20. Canil and O'Neill (1996) point out that charge  
100 balance errors are different between mineral species and increase in the relative order: spinel <  
101 garnet < pyroxene, due to differing amounts of Fe and SiO<sub>2</sub>. Spinel has the highest Fe content  
102 and no Si, which results in  $Fe^{3+}/\sum Fe$  values that are identical (with similar precisions) between  
103 charge balance and Mössbauer (Canil and O'Neill, 1996).

104 In the Dyar et al. (2012) study, three samples (AHUN, G5183, and BBKG) showed  
105 particularly large differences in  $Fe^{3+}/\sum Fe$  (up to 0.93 vs. 0.00) when derived from Mössbauer  
106 spectroscopy vs. when calculated by charge-balance (asterisks in Fig. 1). However, we have  
107 recalculated the data in Table 2 of Dyar et al. (2012) and found errors. These errors are  
108 acknowledged in an erratum (Dyar et al., 2016; this volume) where all *Fe* is reported as total iron  
109 converted to *FeO*. Dyar et al. (2016) also correct sample localities and/or mineral identifications  
110 for 5 garnets from the Adirondack Mountains, N.Y. that we pointed out as unlikely based on  
111 EPMA estimates of  $Fe^{3+}/\sum Fe$ . Our recalculated  $Fe^{3+}/\sum Fe$  values are plotted as white squares  
112 (Fig. 1). After recalculation, samples AHUN, G5183, and BBKG show greatly improved  
113 agreement between the EPMA/charge-balance and Mössbauer spectroscopic methods (Fig. 1).  
114 The difference in  $Fe^{3+}/\sum Fe$  between the charge-balance and Mössbauer methods for the  
115 recalculated dataset is on average 0.06 and the largest is 0.38 (Table 1; Fig 1). To our knowledge,  
116 none of the EPMA data employed garnet standards and we predict that the agreement in Fig. 1  
117 could be enhanced if good garnet standards are developed.

118 Several studies measure  $Fe^{3+}/\sum Fe$  in natural garnet by Mössbauer and report EPMA data,  
119 but do not calculate  $Fe^{3+}/\sum Fe$  by charge-balance (Chakhmouradian and McCammon, 2005;  
120 Kühberger et al., 1989; Locock et al., 1995; McCammon et al., 1998). Many other Mössbauer  
121 studies of  $Fe^{3+}/\sum Fe$  in garnets exist, but mostly investigate synthetic rare-earth-element garnets  
122 (e.g. yttrium-aluminum-garnet), which are considerably different than natural garnets and are not  
123 compared here. We have calculated  $Fe^{3+}/\sum Fe$  from the natural garnets using reported EPMA  
124 values (in some cases back calculating total  $Fe$  from  $FeO$  and  $Fe_2O_3$ ) and compare the results to  
125 their reported Mössbauer determinations of  $Fe^{3+}/\sum Fe$  (Fig. 1). For this suite of garnets there is a  
126 general 1:1 correlation between charge-balance and Mössbauer spectroscopy.

127 There is no reason to expect charge-balance to be more accurate than Mössbauer  
128 spectroscopy. However, if Mössbauer (or a comparable technique) is not available, then charge-  
129 balance calculations are a significant improvement over assuming all  $Fe$  to be ferric or ferrous.

130

### 131 **Implications**

132 We conclude that  $Fe^{3+}/\sum Fe$  estimates in garnet by charge-balance from high-quality  
133 EPMA data provide a suitable alternative to direct measurement of  $Fe^{3+}/\sum Fe$  when Mössbauer  
134 spectroscopy or other comparable techniques are not practical, particularly for Fe-rich species  
135 such as almandine and andradite. These results support the utility of charge balance calculations  
136 for other anhydrous minerals that meet the criteria described here for garnets.

137

138

### **References cited**

- 139 Bajt, S., Sutton, S., and Delaney, J. (1994) X-ray microprobe analysis of iron oxidation states in  
140 silicates and oxides using X-ray absorption near edge structure (XANES). *Geochimica et*  
141 *Cosmochimica Acta*, 58(23), 5209-5214.
- 142 Canil, D., and O'Neill, H.S.C. (1996) Distribution of ferric iron in some upper-mantle  
143 assemblages. *Journal of Petrology*, 37(3), 609-635.
- 144 Chakhmouradian, A., and McCammon, C. (2005) Schorlomite: a discussion of the crystal  
145 chemistry, formula, and inter-species boundaries. *Physics and Chemistry of Minerals*,  
146 32(4), 277-289.
- 147 Droop, G.T.R. (1987) A general equation for estimating Fe<sup>3+</sup> concentrations in ferromagnesian  
148 silicates and oxides from microprobe analyses, using stoichiometric criteria.  
149 *Mineralogical Magazine*, 51, 431-435.
- 150 Dyar, M.D., Agresti, D.G., Schaefer, M.W., Grant, C.A., and Sklute, E.C. (2006) Mössbauer  
151 spectroscopy of earth and planetary materials. *Annual Reviews of Earth and Planetary*  
152 *Sciences*, 34, 83-125.
- 153 Dyar, M.D., Breves, E.A., Emerson, E., Bell, S.W., Nelms, M., Ozanne, M.V., Peel, S.E.,  
154 Carmosino, M.L., Tucker, J.M., Gunter, M.E., Delaney, J.S., Lanzirrotti, A., and  
155 Woodland, A.B. (2012) Accurate determination of ferric iron in garnets by bulk  
156 Mössbauer spectroscopy and synchrotron micro-XANES. *American Mineralogist*, 97(10),  
157 1726-1740.
- 158 -. (2016) Erratum: Accurate determination of ferric iron in garnets by bulk Mössbauer and  
159 synchrotron micro-XANES spectroscopies. *American Mineralogist*, 101, xxx.

- 160 Dyar, M.D., Guidorttri, C.V., Holdaway, M.J., and CoLucci, M. (1993) Nonstoichiometric  
161 hydrogen contents in common rock-forming hydroxyl silicates. *Geochimica et*  
162 *Cosmochimica Acta*, 57(12), 2913-2918.
- 163 Essene, E. (1989) The current status of thermobarometry in metamorphic rocks. Geological  
164 Society, London, Special Publications, 43(1), 1-44.
- 165 Fournelle, J. (2007) Peak Shifts in Al, Mg, Si and Na Ka in Geologically Important Materials.  
166 Fall Meeting Abstracts, 1, 0328. American Geophysical Union, San Fransisco, CA.
- 167 Fournelle, J., and Geiger, C. (2010) An Electron Microprobe Study of Synthetic Aluminosilicate  
168 Garnets. Fall Meeting Abstracts, 1, 2208. American Geophysical Union, San Fransisco,  
169 CA.
- 170 Fournelle, J., and Jonnard, P. (2011) Peak Shift in Mg Ka in EPMA: High Resolution X-ray  
171 Spectrometer Results for Silicate and Oxide Minerals. Fall Meeting Abstracts, 1, 2542.  
172 American Geophysical Union, San Fransisco, CA.
- 173 Garvie, L.A., and Buseck, P.R. (1998) Ratios of ferrous to ferric iron from nanometre-sized areas  
174 in minerals. *Nature*, 396(6712), 667-670.
- 175 Grew, E.S., Locock, A.J., Mills, S.J., Galuskina, I.O., Galuskin, E.V., and Hålenius, U. (2013)  
176 Nomenclature of the garnet supergroup. *American Mineralogist*, 98(4), 785-811.
- 177 Höfer, H.E., and Brey, G.P. (2007) The iron oxidation state of garnet by electron microprobe: Its  
178 determination with the flank method combined with major-element analysis. *American*  
179 *Mineralogist*, 92(5-6), 873-885.
- 180 Johnson, W.M., and Maxwell, J.A. (1981) Rock and mineral analysis. John Wiley & Sons,  
181 Toronto and New York.



- 182 Kühberger, A., Fehr, T., Huckenholz, H., and Amthauer, G. (1989) Crystal chemistry of a natural  
183 schorlomite and Ti-andradites synthesized at different oxygen fugacities. *Physics and*  
184 *Chemistry of Minerals*, 16(8), 734-740.
- 185 Lalonde, A., Rancourt, D., and Ping, J. (1998) Accuracy of ferric/ferrous determinations in micas:  
186 a comparison of Mössbauer spectroscopy and the Pratt and Wilson wet-chemical methods.  
187 *Hyperfine interactions*, 117(1-4), 175-204.
- 188 Li, Y.-L., Zheng, Y.-F., and Fu, B. (2005) Mössbauer spectroscopy of omphacite and garnet  
189 pairs from eclogites: Application to geothermobarometry. *American Mineralogist*, 90(1),  
190 90-100.
- 191 Locock, A., Luth, R.W., Cavel, R.G., Smith, D.G., Duke, M., and John, M. (1995) Spectroscopy  
192 of the cation distribution in the schorlomite species of garnet. *American Mineralogist*,  
193 80(1-2), 27-38.
- 194 McCammon, C., Chinn, I., Gurney, J., and McCallum, M. (1998) Ferric iron content of mineral  
195 inclusions in diamonds from George Creek, Colorado determined using Mössbauer  
196 spectroscopy. *Contributions to Mineralogy and Petrology*, 133(1-2), 30-37.
- 197 McGuire, A.V., Dyar, M.D., and Ward, K.A. (1989) Neglected  $\text{Fe}^{3+}/\text{Fe}^{2+}$  ratios—A study of  $\text{Fe}^{3+}$   
198 content of megacrysts from alkali basalts. *Geology*, 17(8), 687-690.
- 199 Raeburn, S.P., Ilton, E.S., and Veblen, D.R. (1997a) Quantitative determination of the oxidation  
200 state of iron in biotite using X-ray photoelectron spectroscopy: I. Calibration.  
201 *Geochimica et Cosmochimica Acta*, 61(21), 4519-4530.
- 202 -. (1997b) Quantitative determination of the oxidation state of iron in biotite using X-ray  
203 photoelectron spectroscopy: II. In situ analyses. *Geochimica et Cosmochimica Acta*,  
204 61(21), 4531-4537.

- 205 Schingaro, E., Lacalamita, M., Mesto, E., Ventruti, G., Pedrazzi, G., Ottolini, L., and Scordari, F.  
206 (2016) Crystal chemistry and light elements analysis of Ti-rich garnets. American  
207 Mineralogist, 101(2), 371-384.
- 208 Schmid, R., Wilke, M., Oberhänsli, R., Janssens, K., Falkenberg, G., Franz, L., and Gaab, A.  
209 (2003) Micro-XANES determination of ferric iron and its application in thermobarometry.  
210 Lithos, 70(3), 381-392.
- 211 Sobolev, N.V., Schertl, H.P., Valley, J.W., Page, F.Z., Kita, N.T., Spicuzza, M.J., Neuser, R.D.,  
212 and Logvinova, A.M. (2011) Oxygen isotope variations of garnets and clinopyroxenes in  
213 a layered diamondiferous calcsilicate rock from Kokchetav Massif, Kazakhstan: a  
214 window into the geochemical nature of deeply subducted UHPM rocks. Contributions to  
215 Mineralogy and Petrology, 162(5), 1079-1092.
- 216 Valley, J., Essene, E., and Peacor, D. (1983) Fluorine-bearing garnets in Adirondack calc-  
217 silicates. American Mineralogist, 68(3-4), 444-448.
- 218 Wilson, A. (1960) The micro-determination of ferrous iron in silicate minerals by a volumetric  
219 and a colorimetric method. Analyst, 85(1016), 823-827.

220

221 **Figure and Table captions:**

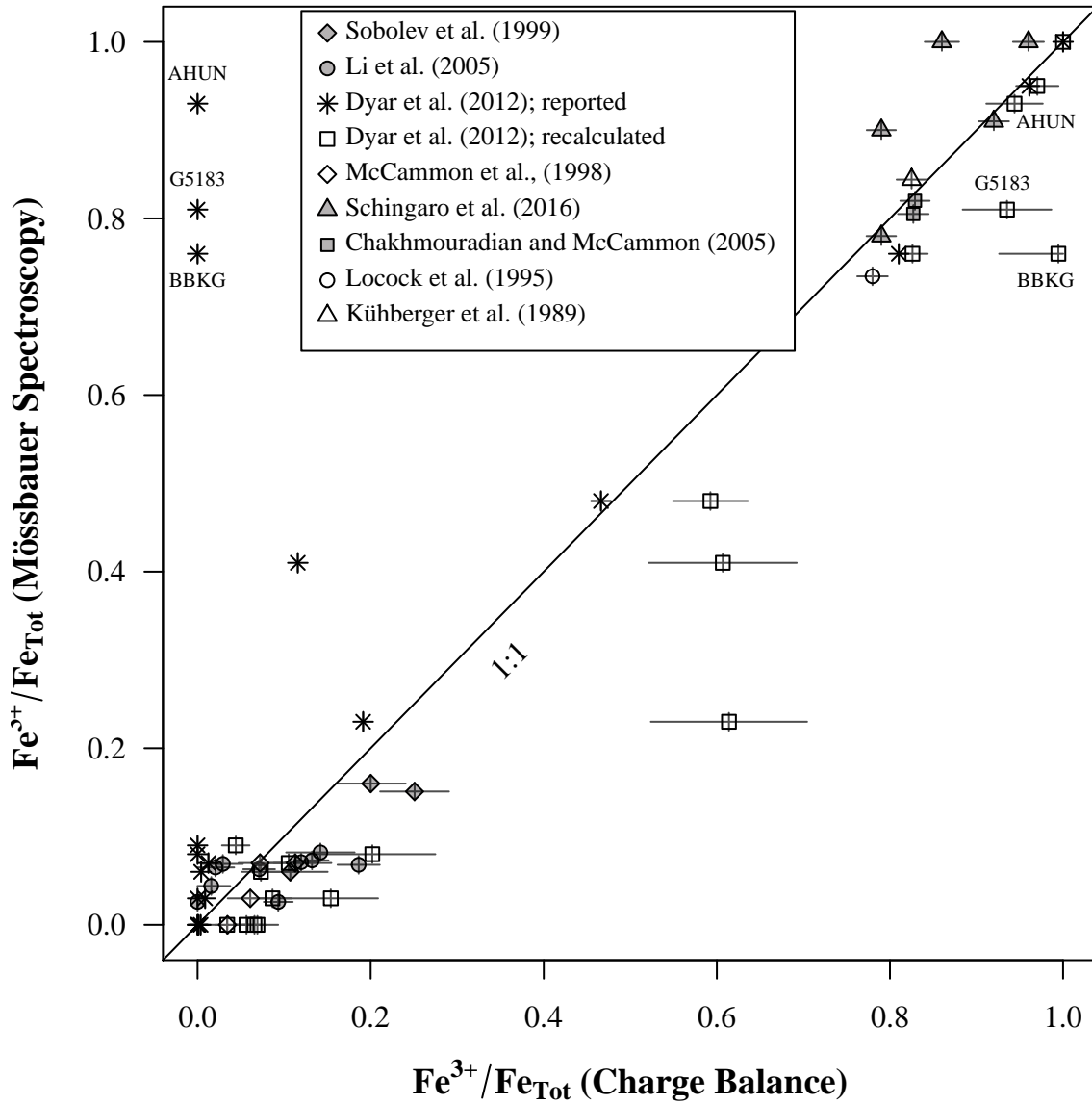
222 **Figure 1.** Comparison of  $Fe^{3+}/\sum Fe$  ratios in garnets derived from electron probe microanalysis  
223 (EPMA) and charge-balance vs. Mössbauer spectroscopy (MS). The error bar size was  
224 calculated by propagating  $\pm 1\%$  of the  $SiO_2$  wt% value through charge balance calculations.  
225 Two data with error bar width of 0 result from the constriction that  $Fe^{3+}/\sum Fe$  can not be  
226 negative or greater than 1. If both the maximum and minimum ends of the error bar  
227 calculation are less than 0 or greater than 1, an error bar of width = 0 results. Error bars for

228 MS values are approximately the size of the data points ( $\pm 0.01$ ). The  $Fe^{3+}/\Sigma Fe$  cation ratios  
229 calculated from the oxide data in Table 2 of Dyar et al. (2012; “reported”) are compared to the  
230 recalculated values in Table 1. Samples AHUN, G5183 and BBKG are labeled.

231 **Figure 2.** Correlation between  $Fe^{3+}/\Sigma Fe$  error and wt% total  $Fe$  in garnets. The magnitude of  
232 error in  $Fe^{3+}/\Sigma Fe$  calculations (y-axis values) were calculated by propagating  $\pm 1\%$  of the  
233  $SiO_2$  wt% value through charge balance calculations. Two data with error bar width of 0 (i.e. y  
234 = 0) result from the constriction that  $Fe^{3+}/\Sigma Fe$  can not be negative or greater than 1. If both  
235 the maximum and minimum ends of the error bar calculation are less than 0 or greater than 1,  
236 an error bar of width = 0 results.

237 **Table 1.** Comparison of  $Fe^{3+}/\Sigma Fe$  determined by electron probe microanalysis (EPMA) and  
238 charge-balance vs. Mössbauer spectroscopy (MS).

239



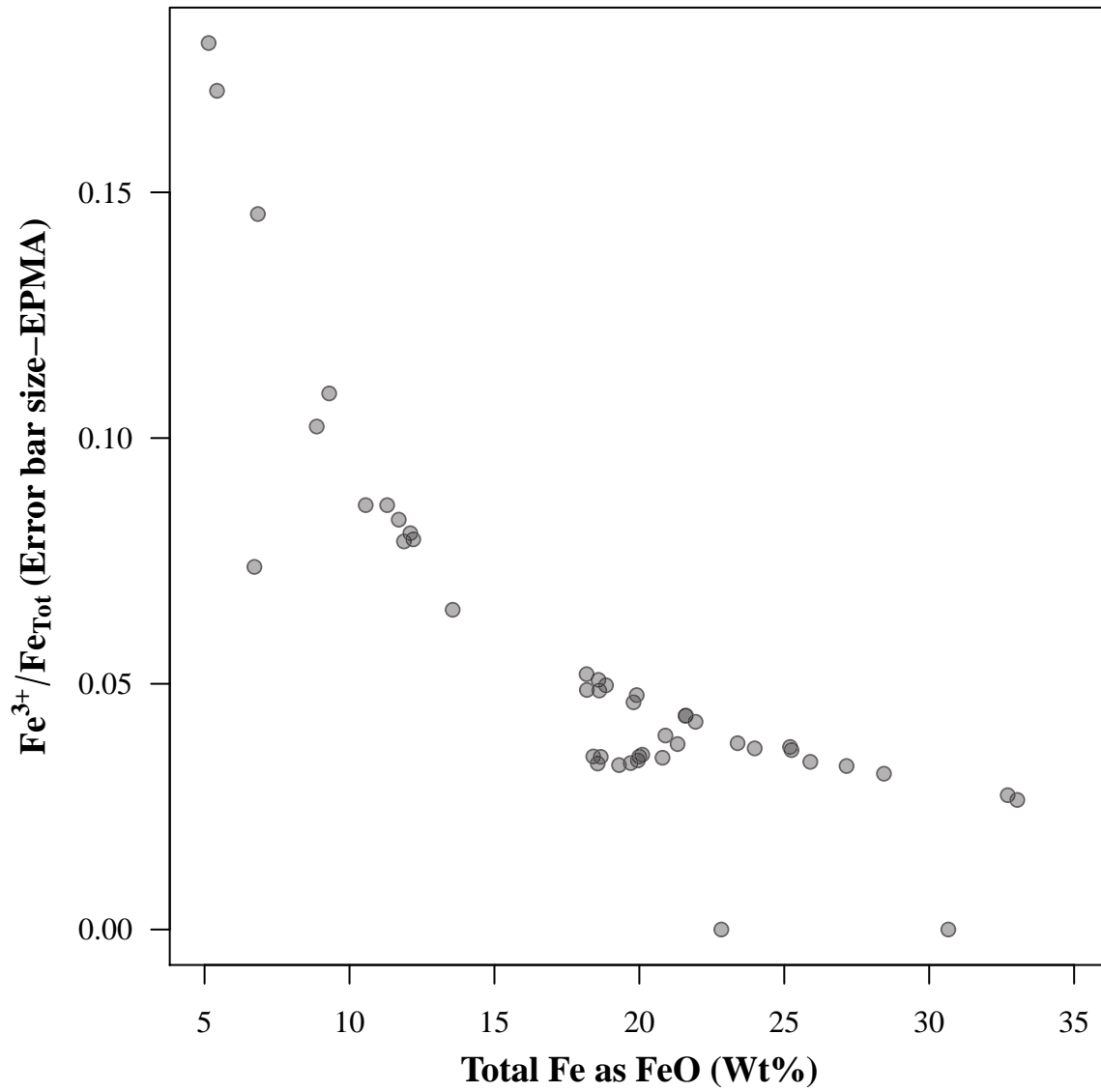


**Table 1:** Comparison of  $\text{Fe}^{3+}/\Sigma\text{Fe}$  determined by electron probe microanalysis (EPMA) and charge-balance vs. Mössbauer spectroscopy (MS).

Sample	SiO <sub>2</sub> (wt%)	Total Fe as FeO (wt%)	Fe <sup>3+</sup> /Σ(Fe) (EPMA) <sup>a</sup>	Fe <sup>3+</sup> /ΣFe (MS)	Fe <sup>3+</sup> /Σ(Fe) diff. (EPMA-MS)	Reference
236-4	40.39	11.30	0.11	0.06	0.05	Sobolev et al. (1999)
237-2	40.39	11.70	0.11	0.07	0.04	Sobolev et al. (1999)
281-2	40.39	12.10	0.20	0.16	0.04	Sobolev et al. (1999)
281-4	40.10	12.20	0.25	0.15	0.10	Sobolev et al. (1999)
97h03	38.16	25.25	0.07	0.06	0.01	Li et al. (2005)
97h06	39.34	22.83	0.00	0.03	-0.03	Li et al. (2005)
97h32	37.39	27.15	0.09	0.03	0.07	Li et al. (2005)
94m44	38.66	21.32	0.02	0.04	-0.03	Li et al. (2005)
94m55	39.15	21.94	0.02	0.07	-0.04	Li et al. (2005)
94m67	37.90	19.80	0.03	0.07	-0.04	Li et al. (2005)
94m80	36.59	23.98	0.12	0.07	0.05	Li et al. (2005)
944010-2	37.48	18.62	0.19	0.07	0.12	Li et al. (2005)
944012-11	38.84	11.88	0.14	0.08	0.06	Li et al. (2005)
97m30	36.71	23.39	0.13	0.07	0.06	Li et al. (2005)
A32W	38.05	6.72	0.99	0.76	0.23	Dyar et al. (2012)
9710	37.32	28.44	0.04	0.09	-0.05	Dyar et al. (2012)
9723	36.58	25.90	0.11	0.07	0.04	Dyar et al. (2012)
9729	36.07	33.04	0.07	0.00	0.07	Dyar et al. (2012)
2A	39.31	19.91	0.07	0.00	0.07	Dyar et al. (2012)
2B	38.86	21.59	0.07	0.06	0.01	Dyar et al. (2012)
8A	38.75	25.20	0.06	0.00	0.06	Dyar et al. (2012)
9B	37.75	10.56	0.59	0.48	0.11	Dyar et al. (2012)
HE1	38.95	21.61	0.09	0.03	0.06	Dyar et al. (2012)
HRM1	36.71	18.19	0.97	0.95	0.02	Dyar et al. (2012)
AHUN	36.52	13.56	0.94	0.93	0.01	Dyar et al. (2012)
G5183	37.58	8.87	0.94	0.81	0.13	Dyar et al. (2012)
ALM	37.01	32.71	0.03	0.00	0.03	Dyar et al. (2012)
G89	38.36	5.43	0.61	0.41	0.20	Dyar et al. (2012)
G17	38.38	5.14	0.61	0.23	0.38	Dyar et al. (2012)
AND	34.52	30.66	1.00	1.00	0.00	Dyar et al. (2012)
1251	41.22	6.84	0.20	0.08	0.12	Dyar et al. (2012)
129	42.00	9.30	0.15	0.03	0.12	Dyar et al. (2012)
BBKG	29.14	20.00	0.83	0.76	0.07	Dyar et al. (2012)
7	39.09	18.59	0.03	0.00	0.03	McCammon et al. (1998)
20	39.11	18.18	0.06	0.03	0.03	McCammon et al. (1998)
55	38.78	18.85	0.07	0.07	0.00	McCammon et al. (1998)
w6	26.73	19.30	0.79	0.90	-0.11	Schingaro et al. (2016)
w12	29.60	20.10	0.96	1.00	-0.04	Schingaro et al. (2016)
w16	27.62	19.70	0.79	0.78	0.01	Schingaro et al. (2016)
nzala	30.10	20.80	0.92	0.91	0.01	Schingaro et al. (2016)
zer2	34.16	20.90	0.86	1.00	-0.14	Schingaro et al. (2016)
AF-05	26.84	18.41	0.83	0.81	0.02	Chakhmouradian & McCammon (2005)
MC-04	25.96	18.56	0.83	0.82	0.01	Chakhmouradian & McCammon (2005)
Ice River Schorlomite	27.15	18.67	0.78	0.73	0.05	Locock et al. (1995)
Schorlomite	28.41	19.95	0.82	0.84	-0.02	Kühberger et al. (1989)

<sup>a</sup> Ratio calculated based on charge-balance calculations.